NATIONAL BUREAU OF STANDARDS REPORT

10028

CORROSION RESEARCH

Progress Report
January 1, 1969 - March 31, 1969
OSW No. 14-01-0001-1091

By

H. C. Burnett
Project Coordinator
Metallurgy Division

To

Office of Saline Water
Department of Interior

U.S. DEPARTMENT OF COMMERCE
NATIONAL BUREAU OF STANDARDS

NATIONAL BUREAU OF STANDARDS REPORT

NBS PROJECT
3120401

NBS REPORT
10028

CORROSION RESEARCH

Progress Report
January 1, 1969 - March 31, 1969
OSW No. 14-01-0001-1091

By

H. C. Burnett
Project Coordinator
Metallurgy Division

To

Office of Saline Water
Department of Interior

IMPORTANT NOTICE

NATIONAL BUREAU OF S
for use within the Government.
and review. For this reason, t
whole or in part, is not auth
Bureau of Standards, Washing
the Report has been specifical

Approved for public release by the Director of the National Institute of Standards and Technology (NIST) on October 9, 2015.

ress accounting documents intended
is subjected to additional evaluation
ire listing of this Report, either in
the Office of the Director, National
r, by the Government agency for which
l copies for its own use.

U.S. DEPARTMENT OF COMMERCE

NATIONAL BUREAU OF STANDARDS

CORROSION RESEARCH

Progress Report
January 1, 1969 - March 31, 1969
OSW No. 14-01-0001-1091

by

H. C. Burnett
Project Coordinator
Metallurgy Division

The Institute for Materials Research of the National Bureau of Standards is engaged in a fundamental study of corrosion phenomena. The program is being conducted by the Metallurgy Division and consists of five tasks. The objective, progress and principal investigators for each of the tasks is reported below.

Task Activities

Task 1 Polarization Studies and Cathodic Protection
W. J. Schwerdtfeger

Objective: To measure by polarization techniques the instantaneous rates of corrosion (computed weight losses) of a series of selected alloys exposed in the laboratory to synthetic sea water. To compare computed weight losses with actual weight losses. To note the effects of such variables as corrodent temperature, aeration and pH. To look for a possible relationship between computed weight and pit depth based on relative apparent areas corroded or based on types of corrosion control (cathodic or anodic).

Progress: All previous work on this project reported by the writer was on experimental data in the temperature range 72° - 80°F. The present data were obtained on iron (same as No. 31 of previous reports) exposed to synthetic sea water at temperatures increased periodically in 3 steps, from 72°F. to 300°F. and then decreased in 2 steps back to 72°F. The sea water was prepared with distilled water and salts added in accordance with specification ASTM D-1141-52.

The iron specimen in the form of a rod (0.5 in. diam) was mounted vertically in the cylindrical chamber of an autoclave. Exposure was to 3000 ml of the corrodent with the waterline at 8 in. from the bottom of the rod. A silver wire (0.05 in. diam) coated with silver chloride served as a reference electrode. The cylindrical inner wall of the stainless steel autoclave was used as the auxiliary electrode. The specimen and reference electrode which protruded through the autoclave head to the outside were insulated by teflon bushings.

The initial polarization measurements were made after 6 hours of exposure and thereafter at times and conditions as tabulated in the table. The air vent referred to in the table terminated in the air space above the corrodent. Total exposure time was a continuous 11 days and 3 hours. The theoretical metal losses are calculated using average corrosion currents for each period between polarization measurements, for example, 52 mg at 96 hours is based on 2500 micro-amperes for 20 hours.

Upon opening the autoclave after 11 days, it was observed that oil had leaked into the chamber from the fan shaft in the head. Except for a few small pits at the bottom end and side of the specimen, most corrosion (pitting) was immediately above the waterline and to a diminishing degree up to one inch above the waterline. Nevertheless, it appears that this corrosion was measured, in view of the reasonable agreement between cumulative calculated (252 mg) and actual (282 mg) weight losses. At 300°F. the vapor pressure was about 50 psi. The corrosion rates (mdd) in the table are based on the metal surface exposed below the waterline. Actually, the corrosion rates in the area where most of the corrosion occurred were several times greater.

The variation of the specimen potential with temperature is considerable. The iron surface exposed to the salt water was dark in appearance. The apparent film formed from the oil may have been a contributing factor in the marked rise in potential, although some rise because of high temperature is to be expected.

Future experiments with iron and other metals or alloys will include the effects on corrosion of changes in oxygen concentration at high temperature.

During the quarter, a manuscript entitled, "Corrosion Rates of Metals, Alloys and Galvanic Couples As Measured by Polarization Techniques", based on O.S.W. project polarization data at room temperature was prepared for oral presentation at the Galvanic Corrosion Symposium, ASTM Meeting at Atlantic City, N.J., June 24, 1969. The manuscript is being offered to ASTM for publication.

Table 1 - Corrosion of iron in synthetic sea water (72° - 300°F)

Exposure time, hrs.	Corrosion Current, μA	Specimen[1] potential, V	Solution temp., °F	Corrosion - metal loss between intervals, mg[2]	Corrosion rate mdd[3]	Remarks
6	320	-0.704	72	2	9.8	Day of exposure Air vent open.
26	240	- .714	72	6	7.3	Air vent open - closed at 28 hrs of exposure.
46	160	- .728	72	4	5.0	Set temp. control for 150° at 49 hrs.
52	900	- .780	150	3	28	Set temp. control for 212° at 54 hrs.
76	3100	- .640	212	50	95	Set temp. control for 300° at 78 hrs.
96	1900	- .164	300	52	58	No change
195	400	- .152	300	113	12	Set temp. control for 212° at 199 hrs.
242	200	- .437	212	15	6.0	Opened air vent at 243 hrs.
245	270	- .470	212	1	8.3	Set temp. control for 72° at 246 hrs.
264	235	- .480	72	6	7.3	Removed specimen at 267 hrs.

[1] Reference electrode, Ag/AgCl. At temperatures above 72°F, the potentials are corrected for reference to 72°F. in accordance with work of S. Greeley, William T. Smith, Jr., Raymond W. Stoughton and M. H. Lietzke - Electromotive force studies in aqueous solutions at elevatd temperatures. I. The standard potential of the silver - silver chloride electrode, J. Physical Chem. 64, 652 (1960).

[2] Based on breaks in cathodic and anodic polarization curves and Faraday's law. Used electrochemical equivalent for Fe=2.8938x10^{-4} g/C. Cumulative wt. loss = 252 mg. Actual wt. loss = 282 mg.

[3] Based on area of specimen exposed to salt water below the water line. Area = 12.7 in^2 (0.82 dm^2).

Task 2 Initial Stages of Corrosion Attack
Dr. A. W. Ruff, Dr. A. Fraker, Mr. D. B. Ballard

Objective: The initial stages of corrosion attack will be studied using electron microscopy and diffraction techniques. Copper-nickel and aluminum-brass and titanium alloys will be studied under conditions approximating use in desalination equipment. Thin-films transmission methods and replica studies will be conducted to determine the relation between sample microstructure and behavior in corrosive media. Lifetime predictions may follow the extrapolation of short time tests.

Progress: Microstructural observation of corroded titanium alloy thin foils continued through this past quarter. Experiments were conducted as described previously to determine the effect of exposure to 3.5 wt. % of NaCl water at increased temperatures and pressures on the corrosion resistance of the materials. The alloys testedand the results are given in Table 1. Electron diffraction studies indicate that the initial oxide covering the titanium surface is a TiO film that is only partially crystalline. Crystals of TiO_2 (anatase)[1] form as the temperature and corrosion times are increased. Another oxide, probably anosovite (Ti_3O_5 or Ti_2O_3-TiO), is found deposited at surface edges and cracks. Less of the deposited form is found as the temperature is increased. The thin oxide film which initially covers the titanium alloys grows somewhat at increased temperatures but begins disappearing as the TiO_2 (anatase) crystals form and grow. At the onset of the TiO_2 crystal formation, their appearance is similar to the TiH_2 particles noted in some corroded and uncorroded specimens.

Figures 1 through 12 show the progress of corrosion on the Ti-0.15Pd alloy as it is taken from the uncorroded state through several testing conditions. Figure 1 is a low magnification electron micrograph showing the grain structure of uncorroded Ti-o.15Pd. Figure 2 shows the same alloy at higher magnification. Figure 3 is a diffraction pattern from this uncorroded alloy. Additional (small) diffraction spots result from a hybride particle in the diffraction area. The absence of any diffraction rings indicates that surface film formation is not advanced. Figure 4 shows the microstructure after corroding for 1 hr. at 100°C and Figures 5 and 6 show the alloy surface after corroding at 150°C and 175°C respectively. Figure 7 is an electron diffraction pattern taken with perhaps some crystalline TiO_2 (anatase) present. Figure 8 is taken from a specimen corroded for 1 hr. at 200°C and Figure 9 shows the microstructure after corroding for 2 hrs. at 200°C. It is apparent that the first film (TiO) is disappearing and that the final film and oxide surface particles are TiO_2 (anatase) which give the crystallite diffraction pattern of Figure 10.

1 The most common titanium oxide, TiO_2 occurs in three forms; anatase; brookite and rutile. These are listed in order of increasing stability, increasing oxygen content and decreasing specific volume. Since rutile is the most stable and adhering form it offers the most protection for the base metal.

Figure 11 is an electron diffraction pattern showing the presence of Ti_3O_5 and Figure 12 shows the morphology of this phase and the manner in which it is deposited.

This set of micrographs just described illustrates the general sequence of corrosion product formation on all of the alloys. Only the rate at which this process takes place appears to differ, varying with changes in alloy composition. The fir t film, TiO, occurs at a later corrosion stage and it disappears sooner on the Ti-0.15Pd alloy than on the Ti-4Al-1Mo-1V and Ti-8Al-1Mo-1V alloys. Electron diffraction patterns show that the oxide covering the surface of all specimens after testing for 2 hours at 200°C in unaerated hot saline water is TiO_2 (anatase) and not TiO_2 (rutile). Corrosion tests are in progress now on the Ti-2Mo alloy and future testing will concern the Ti-2Ni and Ti-6Al-4V alloys. Additional tests involving shorter and longer corrosion times at 100°C and 200°C will be conducted in an effort to learn more about the corrosion products and their relation to alloy composition and testing conditions.

Table 1. Hot Saline Water Corrosion of Ti-0.15Pd, Ti-4Al-3Mo-1V and Ti-8Al-1Mo-1V

Treatment of material (electropolished and corroded in 3.5 wt.% NaCl).	Alloy	Remarks	General Corrosion Sequence
A) 1 hr. at 100°C	1) Ti-0.15Pd	1) Oxide film not detectable by electron diffraction.	
	2) Ti-4Al-3Mo-1V	2) Thin TiO[1] oxide film covering surface.	Formation of initial TiO film.
	3) Ti-8Al-1Mo-1V	3) TiO oxide film is present and it is thicker than that of #2.	
B) 1 hr. at 150°C to 175°C	1) Ti-0.15Pd	1) TiO surface oxide is detected and Ti_3O_5 deposits are found at edges and cracks.	
	2) Ti-4Al-3Mo-1V	2) TiO film has increased and some TiO_2 crystals are present. Ti_3O_5 deposits are found.	Growth of TiO film and onset of TiO_2(anatase) crystalline layer.
	3) Ti-8Al-1Mo-1V	3) TiO film is present and TiO_2 crystals are forming.	Occurrence of deposits of Ti_3O_5 at edges and cracks.
C) 1-2 hrs. at 200°C	1) Ti-0.15Pd	1) TiO surface film is almost gone and diffraction patterns show presence and crystal growth of TiO_2(anatase). No deposits are found.	Decrease in TiO film thickness and increase in the TiO_2(anatase).
	2) Ti-4Al-3Mo-1V	2) TiO film remains, thickness decreased. TiO_2(anatase) has formed and deposits of Ti_3O_5 are occasionally observed.	Deposits of Ti_3O_5 are less frequent.
	3) Ti-8Al-1Mo-1V	3) TiO film remains.	

[1] Further clarification of the identity of this film is in progress.

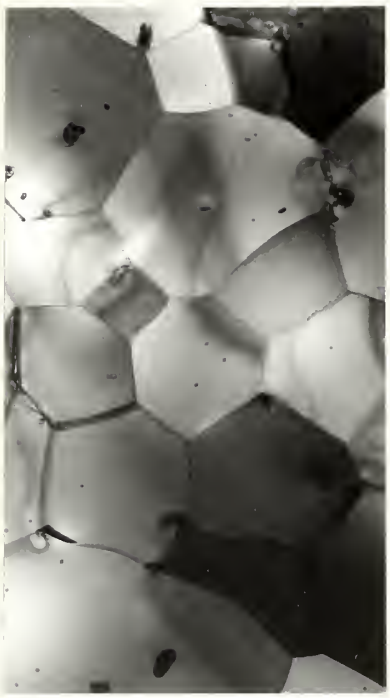

Fig. 1 X4,000
Ti-0.15Pd - uncorroded

Fig. 2 X18,000
Ti-0.15Pd - uncorroded

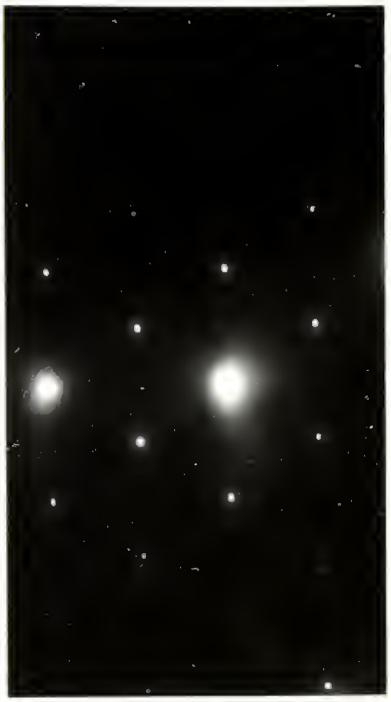

Fig. 3 Diffraction pattern uncorroded Ti-0.15Pd and TiH_2

Fig. 4 X32,000
Ti-0.15Pd - corroded 1 hr. at 100°C

Fig. 5 X32,000
Ti-0.15Pd - corroded 1 hr. at 150°C

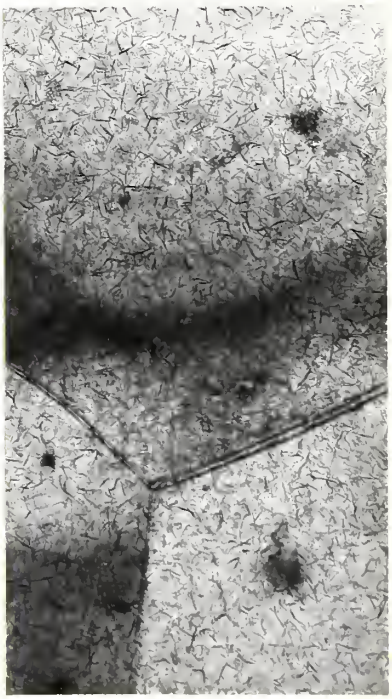

Fig. 6 X32,000
Ti-0.15 Pd - corroded 1 hr. at 175°C.

Fig. 7 Diffraction pattern Ti-0.15Pd and TiO surface oxide of Figs. 5 and 6

Fig. 8 X32,000
Ti-0.15Pd - corroded 1 hr. at 200°C

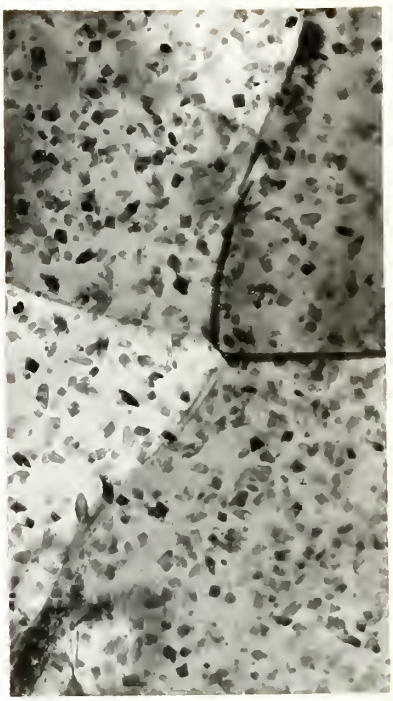

Fig. 9 X32,000
Ti-0.15Pd - corroded 2 hrs. at 200°C

Fig. 10 Diffraction pattern Ti-0.15Pd and TiO_2 (anatase) - corroded 2 hrs. at 200°C

Fig. 11 Diffraction Ti-0.15Pd and Ti_3O_5 deposit - corroded 1 hr. at 175°C

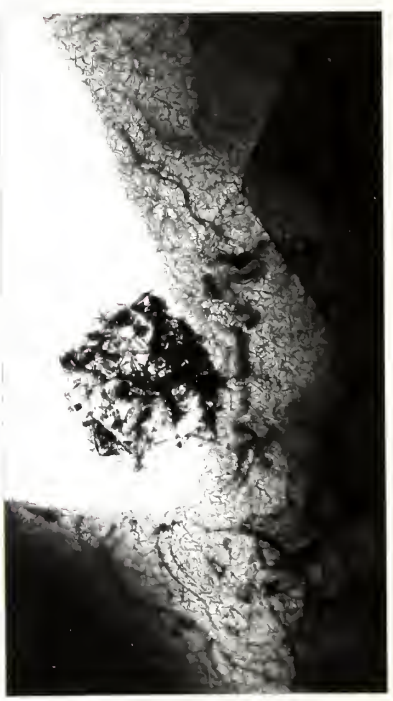

Fig. 12 X12,000
Ti-0.15Pd with deposited Ti_3O_5-corroded 1 hr. at 175°C

Task 3 Spectrometric - Ellipsometry of Films Formed on Iron in Aqueous Solution
Dr. J. Kruger, Mrs. C. L. McBee, Dr. H. P. Layer and John R. Ambrose

Objective: It is proposed to study the electronic properties of the passive films formed on iron by determing their optical constants in the visible region of the spectrum, to determine how these properties are altered by the introduction of chloride ions and other species into the solution that cause passive film breakdown, and to determine how these properties are changed by a change in the atomic arrangement of the metal substrate.

Progress: The objectives of this task encompass the whole gamut of protective film breakdown starting with spectral studies of the nature of the protective passive film, then kinetic and spectral studies of the beginnings of breakdown and finally, holographic studies of the end of breakdown process, pitting. The results obtained on each of these objectives during the last quarter were as follows:

(1) Passive Film Spectra: As explained in earlier reports the formidible part of this study is to obtain unambiguous spectra. Work has continued on a new approach to this problem of multiple values of refractive indices for single wavelengths. The goal is to eliminate those values which may be a result of the computational processes, leaving only single values for each wavelength which may be attributed to the conditions on the specimen surface.

The latest approach to this problem has concerned itself with thickness experiments, as described in the last report. Films are grown at various potentials producing oxide films of increasing thickness as the potential is increased. It is hoped that the various thickness films would have only one set of refractive indices in common, thus eliminating the other multiple values associated with each λ. A number of such experiments have been attempted so far. Growth at potentials o volts, +0.3V, +0.6V and +0.75V produced films of from 5Å to 50Å. The spectra for these experiments, however, did not coincide as closely as would be desirable. The reason for this behavior has not been established as yet, but may lie in the treatment given the surface during the thickness experiments. An oxide film is grown for 1 hr. at a set potential, readings are taken, then the film is reduced back to the substrate values and another film is grown, etc. It was found that the specimen so treated did not produce the same kind of overnight passive spectrum (at +0.75v) as did a specimen that was just reduced to a clean substrate once and then passivated overnight. Figure 1 illustrates this situation using plots of the relative phase retardation, Δ. Thus, it may be possible that the growth and reduction cycles are producing some change on the surface. It will be necessary to produce a surface that does not change before thickness experiments can be successfully utilized to combat the multiple value problem. Since thickness experiments can only be carried out reasonably for short growth times, it is important to determine whether a film grown for 1 hr. (or x hours) at a certain potential would be the same as a film grown for a longer period of time under the same conditions. In Figure 2 a spectrum of the relative phase retardation, Δ for a film grown for 1 hr. at +0.3v is compared with that for a film grown overnight at +0.3V. The

correlation is quite good and indicates that data taken for 1 hr. growth experiments would reasonably be applied to spectra for films grown for >20 hrs.

Further research aimed at interpreting the positive spectra has been carried out in the attempt to choose the correct optical constants for the passive film by comparison with bulk oxide spectra. A crystal of the Fe_3O_4 (artifically grown) was heated for 1 week at 240°C in the presence of air and water vapor. These conditions should oxidize the Fe_3O_4 to γ-Fe_2O_3. X-ray data is being taken to determine whether this is the case. If so, a spectrum for γ-Fe_2O_3 could then be obtained.

In another experiment attempting to classify one of the possible oxides of the passive film (γ-Fe_2O_3 and Fe_3O_4), a specimen was held at +1.25V in the transpassive region for 1 hr. According to previous electron diffraction data the film formed under these conditions would probably be Fe_3O_4. Difficulty with gas evolution from the surface prevented readings below 4300Å and above 5900Å where the reflections are least intense. Figure 3 shows the absorption coefficient spectrum for the transpassive film, for d = 68Å. Multiple values for single λ's are connected vertically. This spectrum does not duplicate the spectrum for bulk Fe_3O_4 reported previously. This fact may indicate that the films grown in solution are actually not comparable to bulk oxide spectra. Further investigations will be needed, however, to determine whether this is the case.

(2) Kinetics and Spectral Studies of Breakdown by Chloride: Previous results of kinetic studies of breakdown by chloride showed the existence of two induction times corresponding to breakdown by chloride.

They also showed no breakdown occurred below a potential labeled E_a^2. During this period both kinetic and spectral studies of films grown below E_a^2 with chloride present were carried out to see if the growth as well as the breakdown process were not affected by chloride below E_a^2.

Figure 4 shows that the growth process of the passive film was the same regardless of whether or not chloride ions were present as long as growth occurred at potentials below the potential called E_a^2. This is the potential observed for the passivation of iron below which ferrous ions were observed in solution while above it no appreciable ferrous ion concentration was observed. Figure 4 also shows that when a film was grown above this potential, there was a marked difference in the growth process as compared to that of a film formed in the presence of chloride. The film continued to grow to much greater thicknesses than the limiting thickness observed when chloride was absent. The chloride produces a different film, which has been shown in the past to contain γFeOOH as well as a cubic oxide. Moreover, it looks as if with chloride present the deposition of ferrous ions is taking place continuously with the production of thick films (>100Å).

An experiment was carried out to characterize the behavior of films grown below the potential E_a^2, i.e. around -0.35V. (vs. SCE) First a film was grown at this potential in the borate solution. A spectrum of Δ is shown for this growth of 1 hr. in Figure 5, curve A. Curve B in the figure indicates a passive film decayed to -0.3V in a previous experiment. The correspondence between the two cases is good. Figure 6, curve C, indicates the effect of a concnetration of (.005N) chloride ion present during the 1 hr. growth period, at -0.35V. The only significant change occurs at 5900Å as shown. For comparison, curve A again shows the growth without chloride present.

(3) Holographic Studies of Pitting: Plans for applying the holographic technique described in the last report to a pitting study were initiated during this quarter. A simple inexpensive potentiostat and a cell were designed which will enable studies of aluminum alloys above and below the critical potential. By means of this potentiostat the potential can be controlled within 1-2 mV. The inception and rate of pitting for long times (up to 1 year) growth will then be studied using the holographic interferometric studies described in earlier reports.

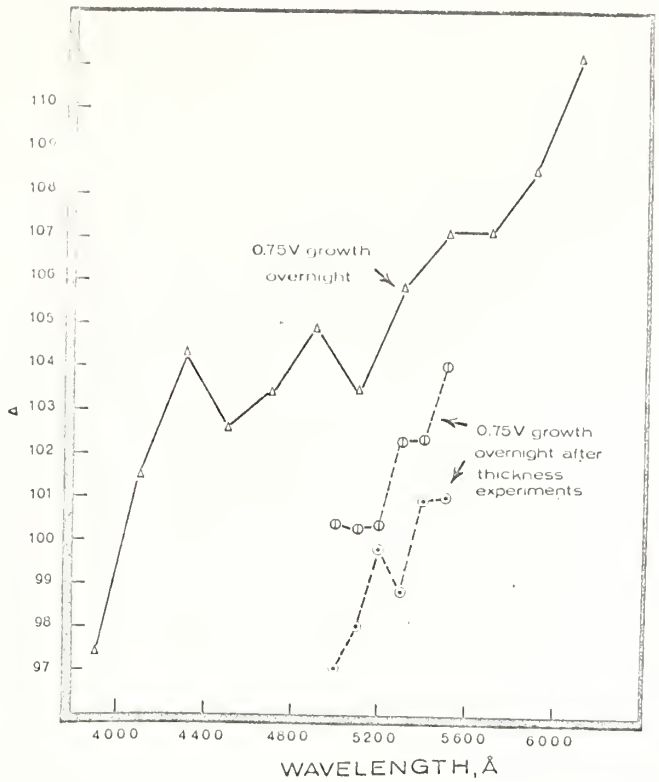

Fig. 1
Comparison of spectra of for passive films grown overnight on surfaces which have undergone thickness experiments with a surface that has just undergone reduction once.

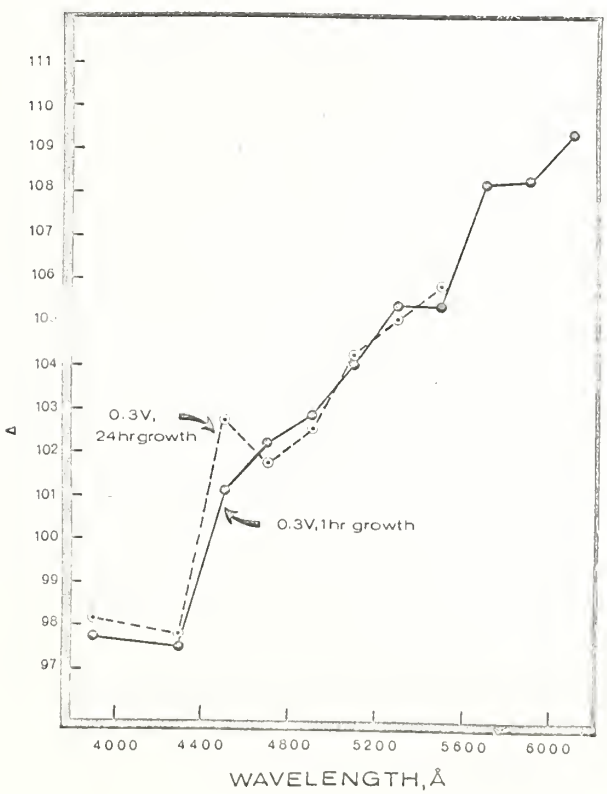

Fig. 2
Spectrum for a film grown just 1 hr. at +0.3V in borate solution compared with a film grown 24 hrs. under the same conditions.

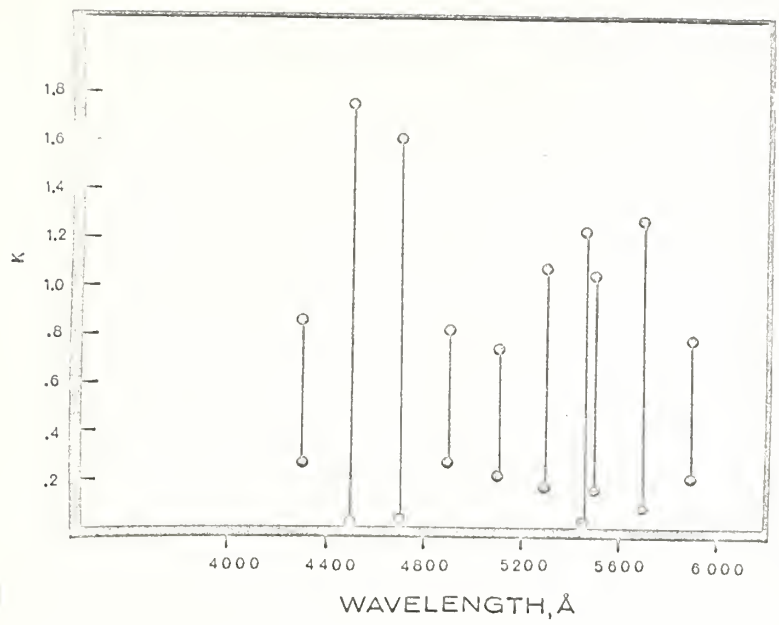

Fig. 3
The absorption coefficient, κ, spectrum for a film grown in the transpassive region at +1.25V.

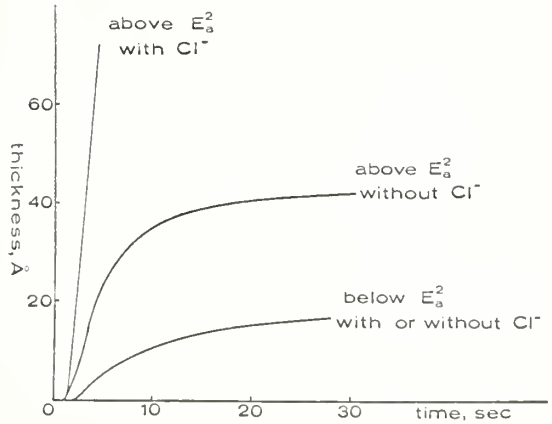

Fig. 4
The effect of potential above E_a^2 (+0.8V SCE) and below E_a^2 (-0.35V SCE) on film growth in the absence and presence of chloride ion (10^{-3}M) in boric acid - sodium tetraborate buffer solution (pH = 8.4). Film thickness was measured by ellipsometry.

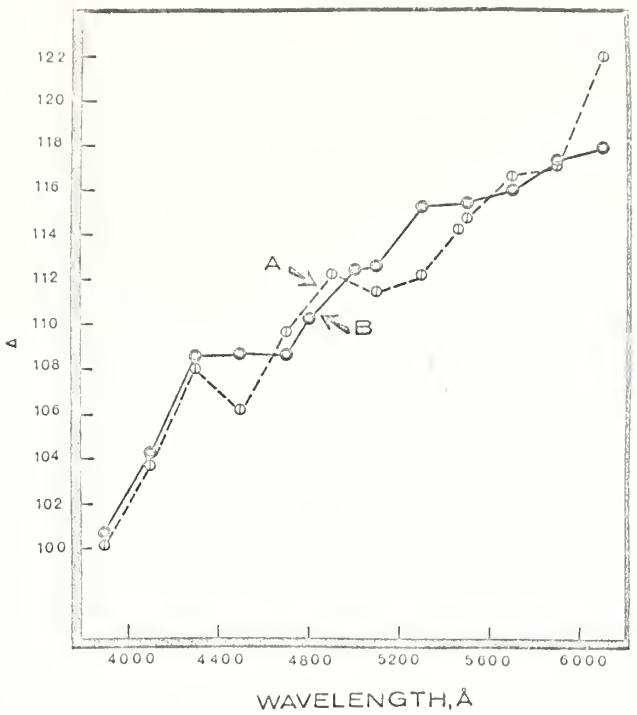

Fig. 5
The spectrum for 1 hr. growth at -0.35V (near E_a^2) is shown in curve A to be almost the same as a spectrum for a decayed passive film, decayed to -0.3V, curve B.

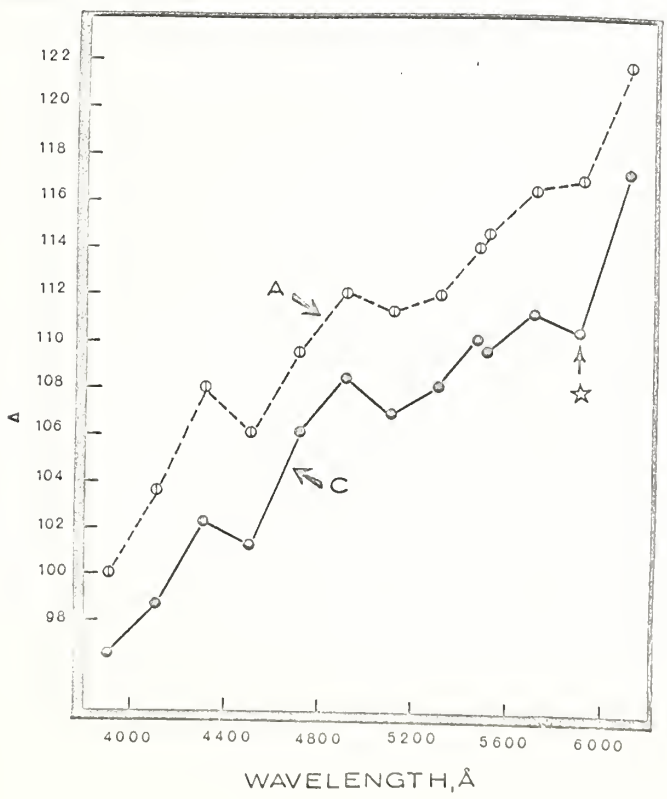

Fig. 6
The spectrum for 1 hr. growth at -0.35V, curve A, in borate is shown in comparison with a 1 hr. growth spectrum for the same potential, with 0.005N chloride ion present in the solution.

Task 4 Structure and Growth Kinetics of Oxide Films on Iron
Dr. A. J. Melmed, and Mr. J. J. Carroll

Objective: Significant progress in understanding surface phenomena can only be expected as the result of several types of investigation on a given problem. Often this is made difficult or uncertain by the fact that each investigation may be done under different experimental conditions. We propose to avoid these uncertainties by combining three surface-study tools into one research instrument (ELF), specifically an ultra-high vacuum instrument which will permit the simultaneous observation of a metal surface by ellipsometry and low-energy-electron-diffraction. The instrument will also have a field-electron-emission microscope built into the specimen region. It is proposed to study simultaneously, during the oxidation of metals by gaseous oxygen, the atomic structure, by the technique of low-energy electron diffraction, and growth kinetics, by the optical technique of ellipsometry.

Progress: The ELF vacuum system is now functioning properly. We have completed a prototype experiment using an evaporated metal film on a (011) - orientated single-crystal tungsten substrate. The tungsten specimen had some carbon contamination as determined by LEED pattern observations. However, n and κ substrate values remained reproducable after repeated high temperature heat treatments of the specimen. The metal was barium; for which optical constants data of evaporated films are available in the technical literature. Our results are shown in Figures 1 and 2. Starting with the tungsten substrate heated to above 2000K in ultra-high vacuum, barium was deposited by evaporation of sucessive doses from a heated iron clad barium wire source, and ellipsometric measurements were made after each dose. Figure 1 shows n and κ, the effective optical constants of the Ba film plus tungsten substrate, as a function of the number of Ba doses (which were not equal doses). Figure 2 shows the optical constants as a function of computed film thickness, assuming that the film optical constants are equal to the limiting values found in Figure 1. It can be seen that the optical constants of the film-substrate combination become approximately constant for film thickness greater than about 400Å, in agreement with the range of thickness values found for other metal films by previous workers. Effective optical constants obtained at high barium film thicknesses appear in good agreement with O'Bryan's work.

We will next repeat this experiment for evaporated iron films, and proceed to investigate the oxidation of such films.

We have experimentally determined that either one or both of the fused quartz ellipsometry windows in the ELF tube are strained. The amount of strain is such that a change of about 10% in the measured optical constants for tungsten occurs as a function of the light beam entry and exit positions. This effects the absolute values of our measured optical constants for (110) tungsten, but does not effect the measurements of relative changes in ellipsometer parameters resulting from reaction of the specimen with oxygen or other gases. We have also tested a new set of fused quartz windows for the new ELF tube being constructed, and found no detectable strain.

An iron crystal of low carbon content was obtained from Corrosion Section personnel. It has been x-ray oriented and is presently being cut by spark-erosion so that specimens can be prepared for our oxidation investigation. This work will be done in the new ELF tube and should proceed in parallel with the work on evaporated iron films in the original ELF tube.

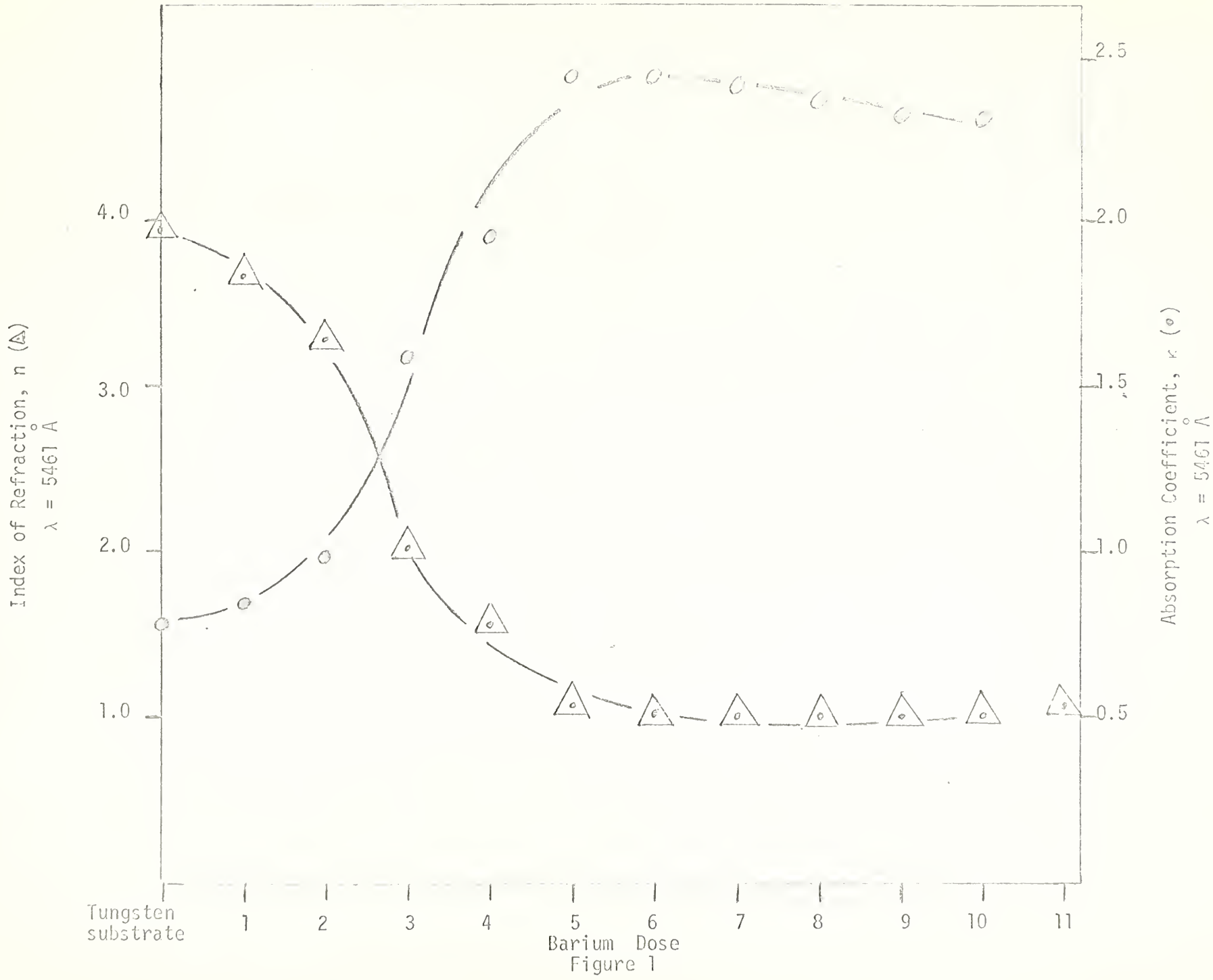
Index of Refraction, n (Δ)
λ = 5461 Å
Absorption Coefficient, κ (o)
λ = 5461 Å
4.0
3.0
2.0
1.0
2.5
2.0
1.5
1.0
0.5
Tungsten substrate
1
2
3
4
5
6
7
8
9
10
11
Barium Dose

Figure 1

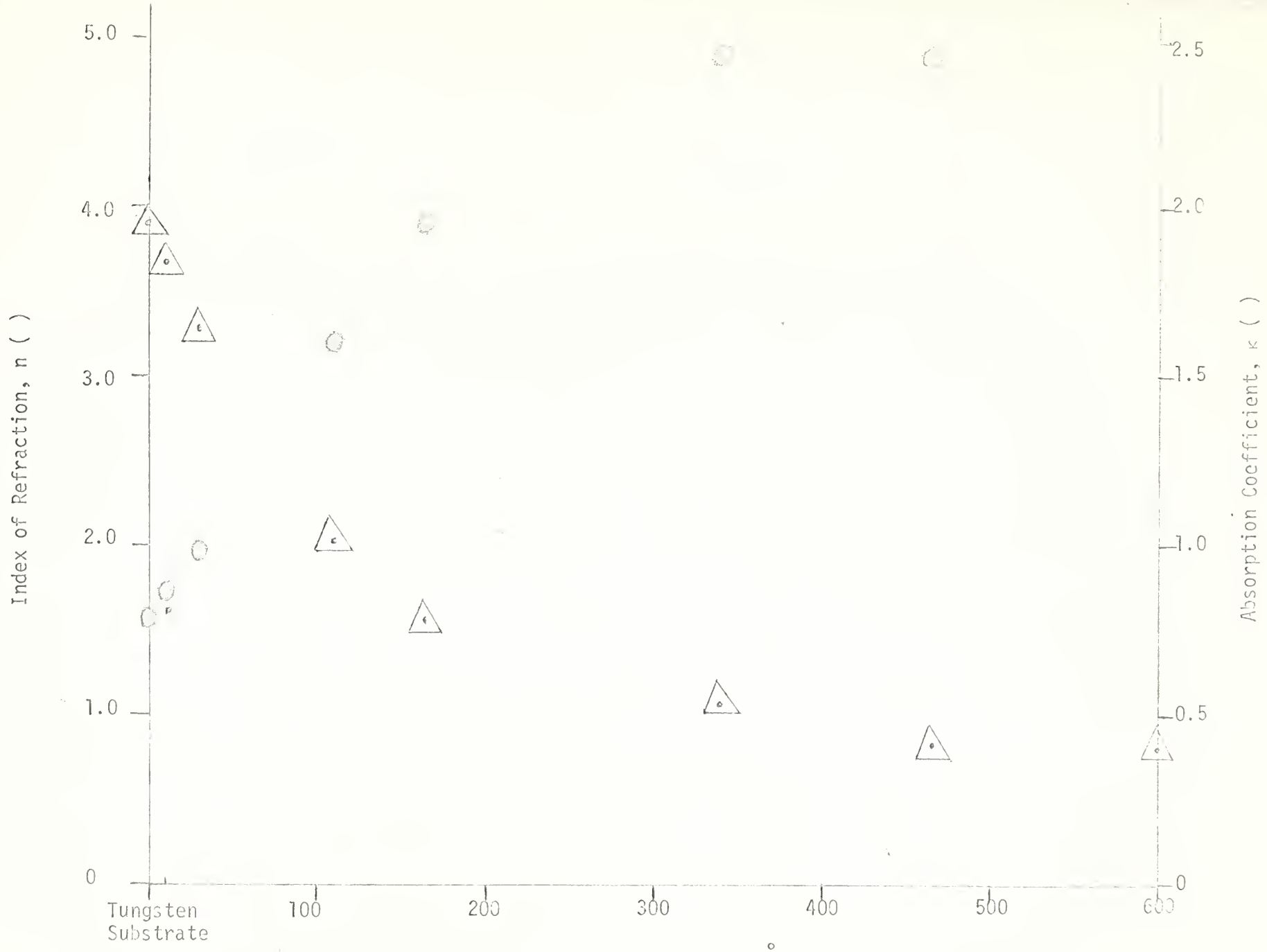
5.0
4.0
3.0
2.0
1.0
0
Index of Refraction, n ( )
2.5
2.0
1.5
1.0
0.5
0
Absorption Coefficient, κ ( )
Tungsten Substrate
100
200
300
400
500
600
Barium Film Thickness (Å)

Figure 2

Task 5 Relation of Corrosion to the Electronic Structure of Alloys
Dr. L. H. Bennett and Dr. L. J. Swartzendruber

Objective: It has been observed that the corrosion rate in sea water of copper-nickel alloys is reduced by the addition of small quantities of iron or manganese. An understanding of this effect, which is as yet unexplained, could lead to the development of more corrosion resistant materials. It is suggested that the effect of iron or manganese on copper-nickel alloys may be to produce a so-called "local moment". It is proposed to investigate this possibility experimentally.

Progress: Further Mössbauer effect studies have been undertaken in the Cu-Ni-Fe system with progress being made on two fronts - in elucidating the constitution as well as the magnetic structure of these alloys. A manuscript "On the Interpretation of Mössbauer Effect Spectra as Related to the Constitution of Cu-Ni-Fe Alloys" has been prepared. In this paper we have identified, for the first time, six different Mössbauer patterns corresponding to iron in six different atomic environments. These include isolated Fe atoms in solid solution in Cu, Fe-Fe and Fe-Ni complexes in solid solution in Cu and Cu-Ni matrices, as well as Fe in precipitates and preprecipitates (Guinier-Preston zones). The effects of annealing, quenching from the solid state, and quenching from the liquid state ("splat-cooled") are shown. Since the presence of different phases with different electrochemical potentials can have important effects on the sea water corrosion of these alloys (see, for example, our earlier paper "The Effect of Fe on the Corrosion Rate of Copper-rich Cu-Ni Alloys", Scripta Met. 2, 93 [1968]), these identifications from the Mössbauer spectra are important.

As noted above in Objective, we have proposed that "local moments" may bear relation to the corrosion of Cu-Ni-Fe alloys. Small amounts of nickel apparently do not form local moments in Cu, but we suspected that the Fe would do so. We have now confirmed this initial suspicion. We have obtained Mössbauer evidence that Fe forms a local magnetic moment, and in fact causes the neighboring Ni atoms to form substantial moments as well. Data as a function of temperature and magnetic field for a Fe source in Cu-30 Ni shows the existence of magnetic clusters of about 5 Bohr magnetons per Fe atom. These studies are being extended to Cu-10 Ni and Cu-20 Ni as well.

A furnace has been put into operation to take Mössbauer spectra above room temperature. Spectra have been obtained to 580°C in a number of samples.

Plans are being formulated to set up magnetic susceptibility apparatus to investigate other magnetic impurities in Cu-Ni alloys.

A copper-5% palladium specimen was corroded in salt water, to compare with the 20% palladium result. Although Cu-20% Pd appeared passive, the Cu-5% Pd corroded very rapidly especially near the edges, where an embrittlement (hydrogen?) occurred. Metallographic and microprobe measurements are underway on these alloys, and new specimens with other compositions are in preparation.